Mechanism of Adsorption of Water in Carbon Micropores As Revealed by a Study of Activated Carbon Fibers

Juan Alcañiz-Monge,*,†,‡ Angel Linares-Solano,† and Brian Rand‡

Departamento de Química Inorgánica, Universidad de Alicante, Alicante, E-03080, Spain, and Department of Materials, University of Leeds, Leeds, LS2 9JT, UK

Received: November 30, 2001

The phenomenon of water adsorption in microporous carbons is investigated using activated carbon fibers as the adsorbents. It is shown that the process of water adsorption is due to both physical adsorption and chemical interaction with surface groups. In accordance with this process, the filling of the micropores is shown to be progressive, the narrower micropores being filled first, and then water is adsorbed in the whole range of microporosity. This study confirms that water adsorbed in the porosity of the carbon has a solid-phase structure throughout the whole range of micropore size and, therefore, the density of adsorbed water has to be considered to be around 0.92 g cm^{-3}.

1. Introduction

The parameters that are used to define the pore structure of activated carbons (ACs) are apparent surface area, pore volume, and pore size distribution, and the characterization of these parameters is critical in assessing their applicability for liquid- or gas-phase processes.[1−3] Physical adsorption of gases is the most common technique for the characterization of porous solids.[1−6] Generally, nonpolar molecules, like N_2, CO_2, Ar, He, CH_4, benzene, and nonane, are used for this purpose.[1−10] Among the gases, N_2 adsorption at 77 K is the most widely used and, usually, has a special status as the recommended adsorptive.[11] On the other hand, polar molecules, like NH_3, H_2O, and alcohols, are scarcely used for this purpose. This is because the adsorption of polar molecules is more complex than that of nonpolar molecules.[12−15] Thus, further studies are needed on the adsorption of polar molecules.

In this work, the focus is on water vapor adsorption, because it has considerable potential due to both the easier experimental conditions (at room temperature the whole range of relative pressures can be realized) and the characteristics of the molecule itself (polar molecule and small kinetic diameter, 0.28 nm). This vapor is used in the characterization of inorganic porous solids, such as zeolites, silicas, and clays.[6,16,17] However, water's interaction with carbon materials (microporous carbons, such as coals, activated carbon fibers, and carbon molecular sieves, and porous carbons like activated carbons) is more complex than that of nonpolar molecules.[18,19] This complexity is due to the weak dispersion interaction of water with graphite, to the tendency of water to form hydrogen bonds with other adsorbed water molecules and surface chemical species, and to the chemisorptive interaction with the mineral matter that may be present in commercial ACs. Most of the studies on the mechanism of adsorption of water by microporous carbons comment on the predominant role of surface groups.[13,14,18−59] Thus, depending on the amount of groups present, water adsorption in these materials starts at lower or higher relative pressures. Some studies have approached the analysis of the role of surface groups (amount and type) by generating them in an oxidative treatment, in many cases with a very strong one (i.e. with nitric acid). However, these treatments may develop a surface chemistry very different from that which commercial ACs normally display (higher and different heteroatom content). For this reason, the influence of pore size in the mechanism of water adsortion is masked by the influence of the surface groups. Thus, the analysis of water isotherms for the characterization of the porosity of carbon materials is not understood sufficiently well.

Recently, a notable development has been the use of computer simulation studies.[60−70] All the molecular simulation were realized on the basis of the Dubinin−Serpinsky concept of primary adsorption sites and the island mechanism of water adsorption.[18,20] Obviously, the simulation results show that the adsorption of water occurs via the formation of three-dimensional clusters centered on oxygenated sites.[67−70] Despite these interesting results, as pointed out by Kaneko,[71] because the contribution of the dispersion force to the whole intermolecular interaction of water is only 24% and the intermolecular interaction cannot be described by the Lennard-Jones potential, it is not easy to simulate the molecular state of water in carbon micropores, and therefore, further experimental analysis is required. Important experimental contributions in this analysis, realized by Iiyama et al.,[72−75] are the in situ X-ray diffraction and small-angle X-ray scattering studies of water confined in carbon micropores.

The work reported here is a study of the phenomenon of water adsorption in microporous carbons, considering the relative influence of the micropore size distribution. For this, activated carbon fibers were used, because they are quite pure (low quantity of inorganic impurities) and the porosity in these materials is well defined (they are mainly microporous solids, with highly uniform slit-shape pores) and, depending on the precursor and activation method, the surface oxygen groups can be limited. The micropore size of the samples has been estimated from the comparative analysis of the adsorption data of N_2 and CO_2.

* Corresponding author. E-mail: Jalcaniz@ua.es.
† Universidad Alicante.
‡ Leeds University.

10.1021/jp014388b CCC: $22.00
Published on Web 03/05/2002

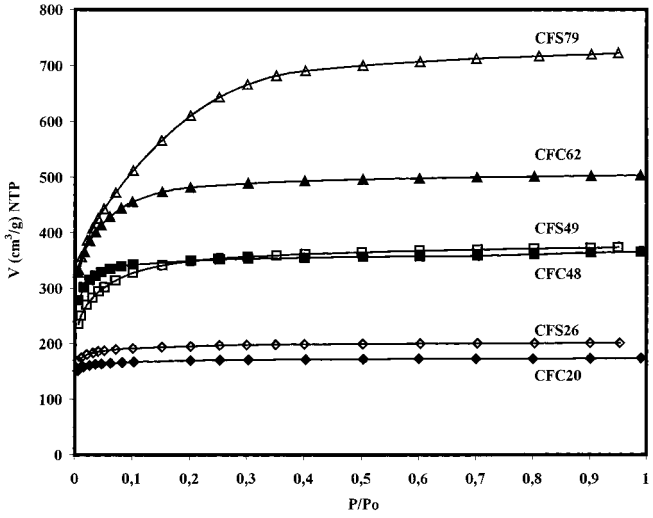

Figure 1. N_2 adsorption isotherms (77 K) of two series (CFC, CFS) of activated carbon fibers.

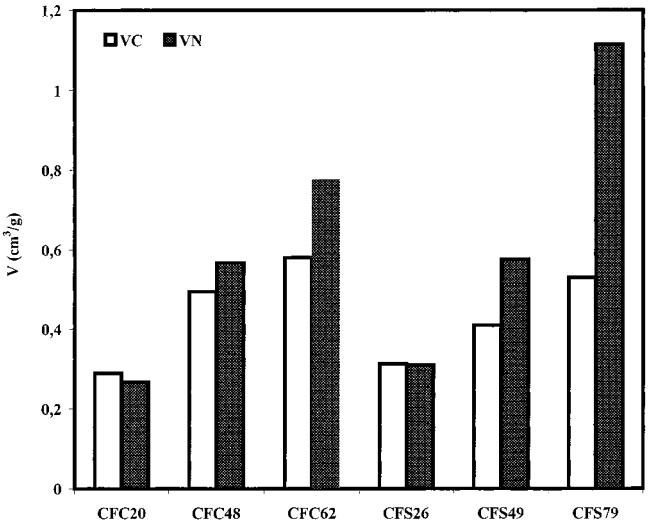

Figure 2. Volume of narrow micropores (V_C) and total micropore volumes (V_N) of the carbons.

2. Experimental Section

Commercial carbon fibers (Kureka) obtained from petroleum pitches were used as raw materials, because they have a lower heteroatom content (these could behave as surface groups) than those obtained from alternatives such as PAN fibers (with high N content, 6−10 wt %) and Rayon fibers (containing oxygen). Activated carbon fibers (ACFs) were prepared by physical activation (thermal treatment in an oxidizing atmosphere), because the fibers develops fewer surface groups than with chemical activation (impregnation with chemicals followed by thermal treatment). Two series of ACF with different degrees of burnoff (number included in the nomenclature) were prepared using CO_2 (CFC) or steam (CFS) as activating gas.

Porous texture analysis of the ACFs was carried out by N_2 adsorption at 77 K and CO_2 adsorption at 273 K (Quantachrome, Autosorb 6). The samples were outgassed at 623 K under vacuum. The Dubinin−Radushkevich (DR) equation[76] was used to calculate the micropore volume. The different pore volumes were calculated as follows:[7] From the CO_2 DR plots (relative pressures < 0.015) the volume of narrow micropores (pore size < 0.7 nm) was obtained. The total micropore volume (pore size < 2 nm) was calculated from the N_2 DR plots (relative pressures < 0.14), which contain the volume of the previous narrow micropores and that of the supermicropores.

Temperature programmed desorption (TPD) was used to characterize the chemical nature of the surfaces of the ACFs. These TPD experiments were carried out in a quartz flow reactor coupled to a mass spectrometer (Micromass PC V.G. Quadrupoles). About 100 mg of sample was heated in a flow of He (60 mL/min) at 20 K/min up to 1173 K.

Water adsorption studies were carried out at 298 K (Belsorp 18). In this case, the samples were degassed at 623 K under high vacuum (10^{-6} Torr). The mechanism whereby water is adsorbed into the micropores was analyzed by characterizing the porosity of the ACFs with a certain amount of water preadsorbed. The water adsorption in a sample was stopped at a certain filling percentage, the bulb was closed, and then the sample analyzed by N_2 and CO_2 adsorption.

3. Results and Discussion

3.1. Characterization of ACF. Figure 1 shows the N_2 isotherms which are of type I (according to the IUPAC classification),[77] indicating that they are essentially microporous solids. The evolution of the isotherms with burnoff (BO) shows a similar tendency in both series. The N_2 adsorption capacity increases with the BO, reflecting the change in micropore volume, while the rounding of the knee demonstrates a widening of the micropores. The steam activation tends to produce ACFs with a micropore size wider than those from CO_2 activation.[7,78,79]

For a more detailed analysis, Figure 2 shows the micropore volumes from N_2 adsorption (V_N) and CO_2 adsorption (V_C). The comparison of the two volumes gives an indication of the micropore sizes.[7] At low BO (around 20%), the two volumes are quite similar ($V_N \sim V_C$) in both series, indicative of a narrow microporosity. In the CFC series, both volumes show a similar increase with the rise of BO (only on sample CFC62 is there a considerable difference). This indicates that CO_2 activation mainly develops both the narrow micropores and the total microporosity. However, in the series CFS, V_C develops with increase in BO to a much smaller extent than the V_N, which increases significantly at high BO. From these observations it is clear that steam activation proceeds through widening of micropores.[7,78]

Considering the elemental composition of the original CF (C and H principally) and the activation method used, the chemical surface species are fundamentally oxygenated groups generated during the activation step. Figure 3 shows the amounts of CO_2 and CO evolved in the TPD experiments. CO_2 is evolved at low temperature as a result of the decomposition of surface groups of acidic nature,[80] whereas the CO comes from weakly acidic, neutral, and basic groups,[80,81] which are more thermally stable and therefore evolve at higher temperatures. The results obtained are in accord with a previous study, with the same precursor materials, by Raymundo and co-workers,[82] which showed large differences between the nature of surface oxygen groups created when the carbon fibers are activated by CO_2 and steam. Steam activation produces a higher amount of oxygen groups, principally evolving CO and therefore being of the weakly acidic or basic character.

In summary, the ACFs obtained are esentially microporous materials with a wide range of micropore sizes (from narrow to wide) and micropore volumes (from low to high) and with different surface oxygen groups.

3.2. Water Isotherms on ACF. Figure 4 shows that the water adsorption isotherms are of type V, a consequence of the low interaction of the water molecules with the graphitic surface.[1,4,18,24,83−85] When the position of the beginning of the isotherm and the knee are located at lower values of relative

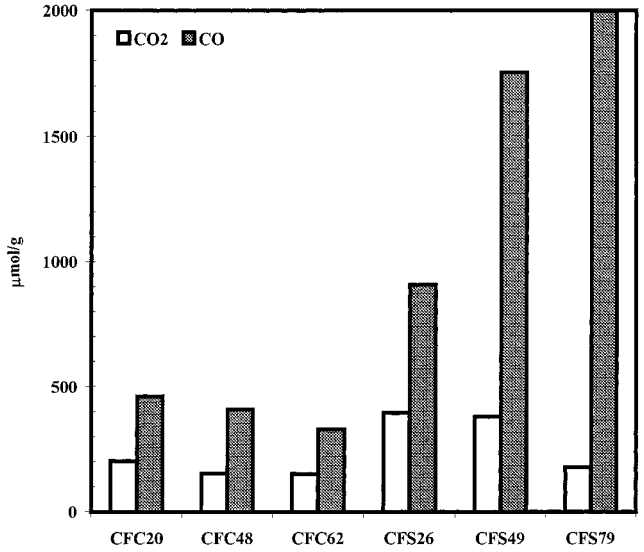

Figure 3. CO and CO_2 evolved during TPD experiments on the ACFs.

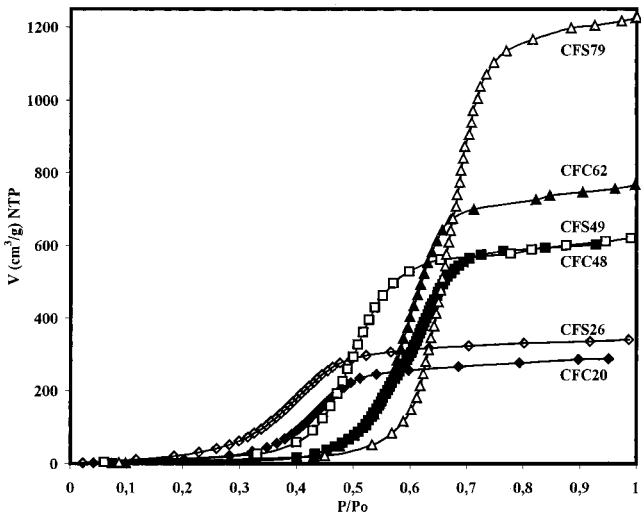

Figure 4. Water isotherms measured at 298 K on the ACFs.

pressures, in both series, the smaller the micropore size is (CFS26 < CFS49 < CFS79; CFC20 < CFC48 = CFC62). This result is reasonable, since the molecule−pore interaction potential increases as the micropore size decreases,[83] favoring water adsorption at the lowest relative pressures. This is in accord with recent molecular simulation results for the water adsorption onto activated carbons, which showed that the pore-filling pressure depends strongly on pore width.[69]

The comparison between the two series suggests that this is not the unique factor that affects the water isotherm shape. Steam-activated samples CFS26 and CFS49, with similar pore widths, respectively, to samples CFC20 and CFC48, show the beginning of adsorption at lower relative pressures. This could be due to their higher content of surface oxygen groups. It is well-known that surface groups promote water adsorption at low relative pressure, acting as primary adsorption centers on which water is retained.[14,18−20,26−28,41−43,48−50,56−59] Nevertheless, the micropore size is also an important factor, as can be seen from the sample CFS49, which has double the concentration of oxygenated groups than CFS26, but water adsorption in this latter sample takes place at lower relative pressures, which must be due to its narrow micropore size. This behavior is shown even more clearly by the sample CFS79, which has the highest content of oxygenated groups of all the ACFs studied, yet water adsorption starts at the highest relative pressure of all samples. This must be caused by its wider micropores. Hence, the starting relative pressure and shape of the isotherm are functions of both micropore size and surface chemical properties (in this case, oxygenated groups). Similar results are found by other researchers,[32,36,42,46,86] who also suggested that micropore size distribution is important in determining the shape of water isotherms. The major or minor influence that oxygenated groups exercise depends principally on the micropore size. This is clear if we consider the overall interaction potential energy (ϕ_T) for a polar adsorbate molecule on a heteropolar surface, which is given by the equation[4,17,87]

$$\phi_T = \phi_D + \phi_P + \phi_F + \phi_{FQ} + \phi_R$$

where ϕ_D = the energy due to dispersion forces; ϕ_P = the energy due to the polar nature of adsorbent and/or adsorptive; ϕ_F and ϕ_{FQ} = the energy due to permanent dipole and quadrupole moments of the adsorptive molecules, respectively; and ϕ_R = the energy due to repulsion forces.

The terms ϕ_D and ϕ_R are the nonspecific contributions that are always present in physisorption, whereas the other terms provide the specific contribution that may be important to the overall adsorption energy according to the polar nature of the molecules and the adsorbents.[88,89] For very narrow micropores (<0.7 nm), the adsorption potential is principally controlled by the higher dispersion forces of the two micropore walls, so the effects of other other terms are not significant. For medium-sized micropores (0.7−1.2 nm), the dispersion force term decreases strongly with the increase in micropore size, so its contribution to the overall adsorption energy is less and, hence, the effect of terms ϕ_P, ϕ_F, and ϕ_{FQ} (which are a function of surface groups) is more appreciable. For wider micropores (>1.2 nm), the results suggest that the influence of surface groups is scarce, even though their concentration is high. Here the dispersion forces are weak, and so adsorption only happens at high relative pressure. The interaction of water with the surface groups should be favored at low relative pressures. Perhaps the accessibility of water from the exterior into the micropore structure is driven mainly by the dispersion forces. Finally, both series show similar trends between the saturation volumes for water adsorption (Figure 4) to those recorded for nitrogen at 77 K (Figure 1), which correspond to the total micropore volumes in the samples. Table 1 lists the micropore volume from both nitrogen and water adsorption isotherms, assuming, as is usual, that the adsorptives are in the liquid state (liquid density 0.808 g cm^{-3} for nitrogen and 1.0 g cm^{-3} for water). This table contains the ratio of both volumes, which should be approximately unity according to the Gurvitsch rule.[4] As is normally observed, the water volume is lower than the nitrogen saturation volume.[14,15,33,34,36,37] This ratio varies remarkably from one sample to another, in many cases being around 0.5−0.9. From this discrepancy it has been suggested that the density of water in the adsorbed phase is lower than that of the normal

TABLE 1: Micropore Volumes Deduced from N_2 and H_2O Adsorption and the Ratio between Them[a]

	V_{N_2}, $cm^3\ g^{-1}$	${}^{L}V_{H_2O}$, $cm^3\ g^{-1}$	${}^{L}V_{H_2O}/V_{N_2}$	${}^{S}V_{H_2O}/V_{N_2}$
CFS26	0.31	0.27	0.88	0.96
CFS49	0.58	0.50	0.86	0.95
CFS79	1.12	1.00	0.89	0.97
CFC20	0.27	0.23	0.85	0.93
CFC48	0.57	0.49	0.86	0.94
CFC62	0.78	0.71	0.91	0.99

[a] Definitions: ${}^{L}V_{H_2O}$, micropore volume using liquid density of water; ${}^{S}V_{H_2O}$, micropore volume using solid density of water.

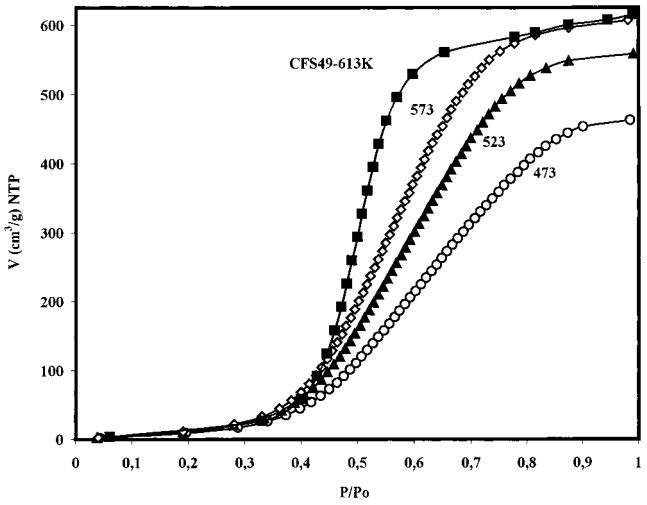

Figure 5. Effect of outgassing temperature on the shape of the water isotherms of sample CFS49.

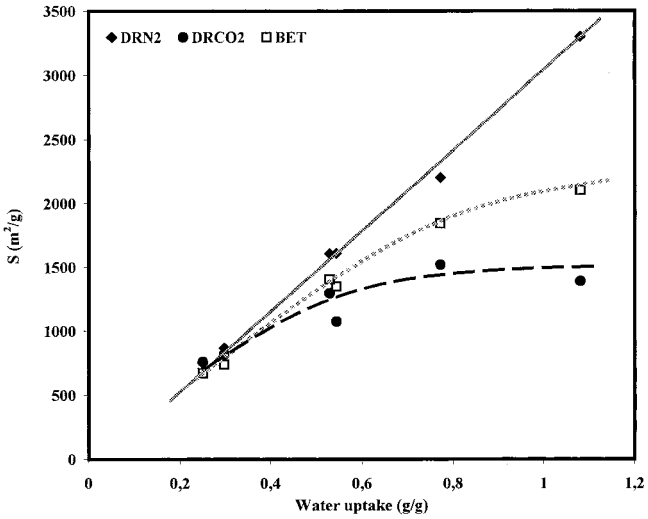

Figure 6. Total amount of water adsorbed vs apparent surface areas of ACFs deduced from N_2 adsorption (by BET and DR methods) and from CO_2 adsorption at 273 K (by DR).

liquid at the corresponding temperature. Sing suggested that this may occur as a result of the hydrogen-bonding propensity of water.[4] Another possibility, more reasonable for the low ratios (low water volumes), is that water does not completely fill the micropore volume. This could be caused by the low surface polarity of the carbons, which controls the wetting of the pore walls and subsequent spreading of the adsorbed water film.[40] This point will be analyzed in the next section.

3.3. Assessment of the Density of Water Adsorbed in Micropores. An important consideration in the study of water adsorption is the experimental conditions used: outgassing temperature and the level of vacuum attained. As Hassan[90] showed for a given sample, there can be large discrepancies in the uptake values between different authors, which are attributed to the different experimental conditions used. A significant effect of outgassing temperature on the shape of water isotherms was also observed in the present study. The samples take up less water when degassed at low temperature than at high. This reduction can be caused by a blockage of the micropore entrance by strongly adsorbed water molecules, which hinder the process of micropore filling.[91,92] This effect is more enhanced on CFS49, which has relatively narrow pores and a high concentration of surface groups (see Figure 5). On the other hand, for CFS79, despite having a high concentration of surface groups, this effect is less marked because it has wider micropores on average. This can explain the experimental results obtained from other researches that give a low micropore volume from water adsorption.[15,34] To overcome this, all experiments here were carried out with samples previously degassed at 613 K. However, on all samples the micropore volume obtained with water adsorption is still lower than that from nitrogen adsorption.

A possible explanation for the low micropore volumes obtained from water adsorption could be that the amount of water adsorbed is more closely related to the surface area than the pore volume. To check this, the amount of water adsorbed (grams of water/grams of sample) can be compared with the specific surface area, either from the application of the BET method to N_2 isotherms or the DR method to N_2 and CO_2 isotherms (Figure 6). The amount of water adsorbed only shows a linear relationship with the BET and DR−CO_2 surfaces at low values of these. In contrast, there is a linear relationship for all values of the surface area obtained from the DR interpretation of the N_2 data. It is well know that the DR method gives an overestimation of the surface when the pores can accommodate more than two adsorptive layers, which often happens with N_2 adsorption. Thus, this actually represents the micropore volume. Hence, the amount of water adsorbed is directly related to the total micropore volume, suggesting that the water adsorption in the micropores is achieved through a filling mechanism of all this volume. This is not the case when the DR equation is applied to CO_2 adsorption, because at 273 K and at subatmospheric pressures the CO_2 relative pressure used is low.[7] Another interesting point that we can extract from this figure is the fact that, if it is assumed that water does not fill the microporosity because of the pore entrance blocking effect, this must be independent of micropore size, since the linearity covers all the range of micropore size. This does not seem to be reasonable.

To explain why a lower micropore volume is always obtained with water adsorption than with nitrogen adsorption, the pore texture of samples saturated with water was further analyzed by adsorption of N_2 at 77 K and CO_2 at 273 K. From this, we can check whether the adsorbed water completely fills the micropore structure. This free pore volume (in which hypothetically water does not adsorb) is considerable in the highly activated samples. For example, on CFS79 this should be 0.13 cm^3/g, which represents an appreciable amount of nitrogen to be adsorbed and can be measured easily. The results show that none of the ACFs saturated with water show any N_2 or CO_2 adsorption, which indicates that all the micropore structure is filled with water.

However, there is still the possibility that a fraction of the micropore volume is not occupied by water, because the pore entrances are blocked by the adsorbed water and this hinders the entry of N_2 and CO_2. To analyze this point, the same experiment was carried out on ACFs with a fractional uptake of water (80−90 wt % of the saturated water adsorbed), as is shown for sample CFS79 in Figure 7 as an example. During the realization of a water isotherm, the adsorption of water was stopped at a predetermined relative pressure, Pr (closing the bulb). Next, this hydrated sample was cooled and its pore structure analyzed by gas adsorption. The same procedure was realized on all samples covering a wide range of fractional water uptake. A similar procedure was carried out by Stoeckli and Huguenin.[93] On all ACFs, the water adsorbed is still high but the possibility of pore blocking is reduced. Additionally, this type of experiment will be useful for the study of the mechanism of water adsorption in these materials.

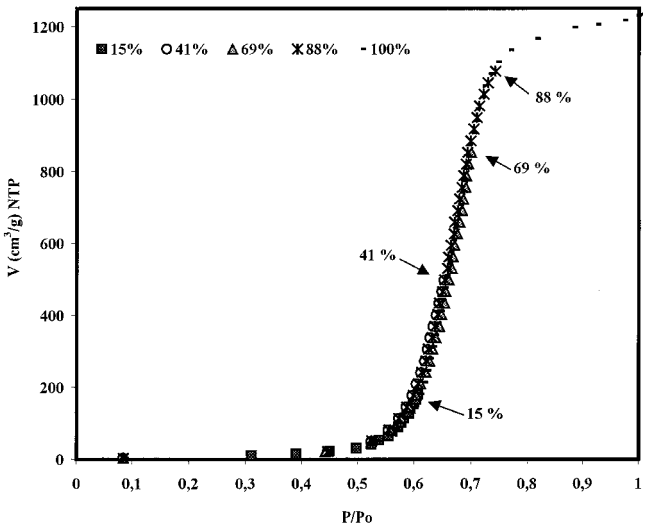

Figure 7. Water adsorption isotherms (298 K) of sample CFS79 at different extents of water filling (wt %).

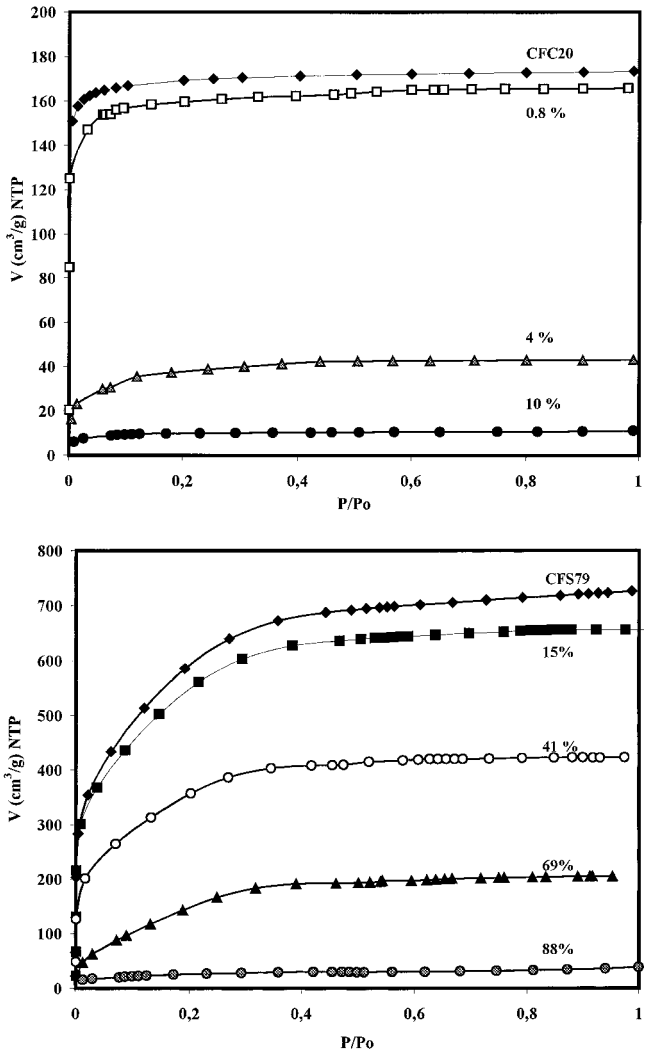

Figure 8. N_2 isotherms (77 K) of ACFs at different extents of water uptake (wt %): sample CFC20 (a) and sample CFS79 (b).

Figure 8 shows the nitrogen isotherms for two representative samples with different degrees of water adsorbed, one with narrow micropores (CFC20) and the other with wider micropores (CFS79). It is important to note that there is still significant nitrogen adsorption on samples with an amount of preadsorbed water near to the saturation value. A reduction in the amount of nitrogen adsorbed is observed on all samples after water adsorption, which is more noticeable as the fraction of water adsorbed increased. Samples with medium or wide micropores show similar behavior to CFS79 (Figure 8b), in that there is a reduction in N_2 adsorption proportional to the amount of water adsorbed. On the other hand, on samples with narrow micropores (Figure 8a) there is a larger reduction in the nitrogen adsorption than corresponds to the volume of water adsorbed. In fact, the adsorption of only 4 wt % of water on sample CFC20 causes a reduction on N_2 isotherms of around 75%, and with 10 wt % of water adsorbed this reduction is very close to 100%. However, in the same situation, the reduction in the CO_2 isotherms is proportional to the amount of water preadsorbed. Hence, this behavior, which is only shown on samples with narrow micropores, is due to the well-known diffusional problem of the N_2 molecules entering the narrow pores. This behavior was also found with CMS by other researches, in which the diffusivities of nitrogen decrease dramatically with small amounts of adsorbed water in the micropores.[94,95] From these results, it can be deduced that the initial water adsorption takes place at the pore entrances, where it is expected that the oxygenated groups are located.[96,97] The same behavior could take place during the determination of a water adsorption isotherm when the concentration of surface groups is high and the pore size is narrow, which can explain the effect of outgassing temperature on the water isotherm (Figure 5).

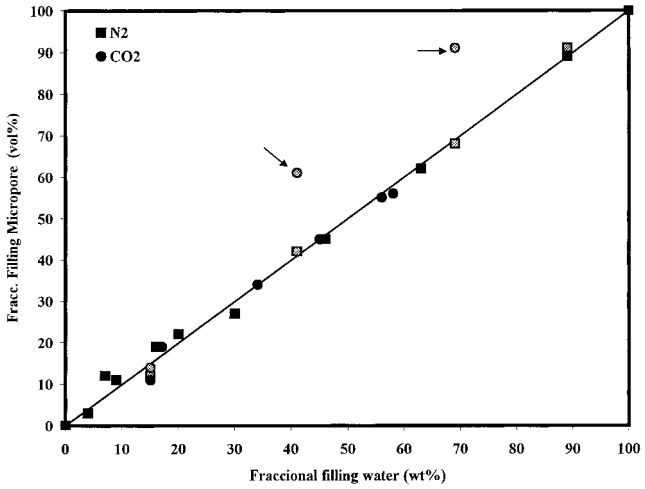

Figure 9. Fractional water adsorbed vs the fractional micropore filling of CFS79 (gray) and the rest of the ACFs (black) from N_2 (□) and CO_2 (○) adsorption.

The overall micropore volume and the volume of narrow micropores on ACFs partially filled with water was calculated from the N_2 and CO_2 isotherms, respectively. In the case of samples with diffusional limitations (CFC20 and CFS26), the micropore volumes from N_2 were not considered. To find a relationship between the amount of water adsorbed and the decrease in apparent micropore volume, the fractional water adsorbed (i.e., the weight of water adsorbed at relative pressure P/P_0 vs weight of water adsorbed at saturation) and the fractional micropore filling ($1 - V_r/V$), where V_r = micropore volume on sample partially hydrated at P/P_0 and V = micropore volume of the fully degassed sample, were calculated. With this procedure, it is possible to correlate all the results obtained with the different ACFs, which cover a significant range of micropore volumes and capacities of water adsorption, as shown in Figure 9.

Figure 9 shows a linear relationship between the fraction of water adsorbed and the fractional micropore filling, which covers

both low and high values of fractional water adsorbed. In the latter case the results show that there is not an unoccupied micropore volume. The observed reduction in micropore volume accessible to N_2 and CO_2 is only a result of the volume of the water preadsorbed. These results allow a calculation to be made of the density of the adsorbed water (at least relative to that of the adsorbed nitrogen and carbon dioxide). The linear relationship indicates that the density of water adsorbed is not a function of the fractional filling of the pore volume or the micropore size. The density calculated is around 0.90−0.92 g/cm^3, which is very close to that of ice I, 0.917 g/cm^3. It should be noted that, in principle, this value is to be expected, because the characterization of the porosity on samples partially hydrated was carried out at 77 and 273 K, for N_2 and CO_2 adsorption, where the stable phase is ice I. Therefore, the question to be answered is, what is the phase of water adsorbed at 298 K?

X-ray and neutron diffraction studies by Iiyama et al.[73]and Bellisesent-Funel et al.[98] showed that adsorbed water has a solidlike structure, even at 303 K, and they could not observe a clear phase transition over the temperature range 143−303 K. Recently Kaneko et al.,[99] also came to the same conclusion, suggesting that the water confined in micropores is very similar to bulk ice. Other studies related to this applied the DTA[98] and the DSC[100,101] techniques to the analysis of the freezing behavior of water adsorbed in microporous carbon, when cooled from 300 to 77 K and from 303 to 123 K, respectively. In both cases, it was observed that water adsorbed in carbon micropores does not freeze. This could be due to the fact that the water adsorbed at 303 K already has a solidlike structure.

In addition, from the analysis of Figure 9, we can form the same conclusion. If water adsorbed at 298 K is considered to be liquidlike, it would occupy a micropore volume related to its liquid density. When the sample, partially filled with water, is further characterized at 77 or 273 K, the liquid water would transform to the solid state with a consequent change in density and in the occupied volume, which would increase by about 9% of the occupied volume at 298 K. In this situation, the ratio of the fractional filling of micropores to the fraction of water adsorbed would become higher than unity. At high values of fraction filling by water adsorbed (90%), the total porosity should become occupied. This is not observed in Figure 9, and there is still space for N_2 and CO_2 adsorption. Hence, it can be concluded that the adsorbed water was already in the solid state at 298 K.

Using this new density value, the volumes obtained for the water adsorption are quite similar to those determined from N_2 adsorption (Table 1). The values show that as the pores are widened, the ratio becomes closer to 1. This probably reflects an arrangement of water molecules inside the micropores,[40,95] which better corresponds to that of bulk ice rather than the more constrained environment in the molecular-sized pores.

3.4. Study of Mechanisms of Water Adsorption on the Microporosity. The comparative analysis of the water isotherms (Figure 4) and the textural characteristics and surface chemistry of the different ACFs (Figures 2 and 3) have already shown that the adsorption of water depends on both micropore size and surface groups. On the other hand, the amount of water adsorbed at saturation obtained in diverse ACFs showed a clear correlation with the volume of total microporosity (Figure 6).

The study of N_2 adsorption in the partially hydrated ACFs (CFS26 and CFC20) (Figure 8a) reveals that the water molecules adsorb initially in the micropore entrances. This can only be due to the interaction between the water molecules and the oxygenated groups located here, because the dispersion forces between water and carbon are weak. In addition, these experiments, enable some conclusions to be made about the mechanism of water adsorption in micropores. Figure 9 demonstrated that water adsorption in the micropores is through a progressive and complete filling of this volume. When the sample CFS79, partially filled with water, is cooled to 273 K and CO_2 is adsorbed, it is observed that the micropore volume decreases more than expected (41 wt % of adsorbed water causes a reduction of 61% on the V_C, Figure 9). This behavior cannot be attributed to micropore blocking, since the N_2 adsorption, for the same fractional water adsorption, gives a proportional decrease in the total micropore volume. Therefore, it seems that the decrease in the narrow micropore volume is due to water filling. The analysis of the nitrogen isotherms (Figure 8b) also shows this feature, since the beginning of the nitrogen isotherm is related to the filling of narrow micropores, while the knee is related to filling of the wider micropores. As the fractional water adsorption increases, there is a greater decrease in the initial point of the isotherm than in the knee (the relationship between the volumes at the initial point of the isotherm and at saturation varies from 0.39 to 0.3 in the sample with 41 wt % of adsorbed water and then to 0.11 with a fractional water adsorption of 67 wt %). This indicates adsorption of the water in narrow micropores at low relative pressures.

CFS79 is the only sample to display this behavior, because it has a significant difference between the amounts of each type of microporosity (Figure 2). Thus a fractional water adsorption of 50 wt % is sufficient to fill the whole of the narrow micropore volume. This feature is clearly seen in the DR representation of the N_2 isotherms of CFC62 and CFS79 (Figure 10). For sample CFC62, as the amount of water adsorbed increases, there is a similar decrease in the DR curve over the whole range, i.e., its form hardly changes. On the other hand, the DR curve for CFS79 shows a remarkable change in shape at high values of fractional filling, which is predominantly in the range of low relative pressures, characteristic of the filling of narrow micropores. This behavior is more easily observed on a sample with a wide micropore size distribution.

It is now possible to comment on the extent to which water adsorption is distributed homogeneously over the micropore surface, preferentially in micropores of a certain size, or is centered in the micropore walls with high concentrations of functional groups, and in this regard a comparison of the adsorption of both N_2 and CO_2 is informative.[7] To allow for the different adsorption temperatures, the results were corrected for adsorption temperature and the physicochemical characteristics of the adsorptives by plotting the Polanyi characteristic curves and applying the DR equation.[4,76] According to Dubinin−Polanyi, the data for the adsorption of different vapors onto a single adsorbent corrected for molecular volume should coincide on a unique curve: the characteristic curve. The characteristic curves are the plot of the logarithm of the volume of liquid adsorbed versus the square of the adsorption potential corrected for the affinity coefficient of the adsorptive $((RT/\beta \ln(P_0/P))^2$, where β is the affinity coefficient.[102,103] Figure 11 shows the characteristic curves of samples CFS79 and CFS79 with 41% saturated with water. The β and density of both adsorptives were based on a previous study.[102]

Inspection of the N_2 adsorption curve for CFS79 shows the common feature of a large deviation downward for values of $(A/\beta)^2$ higher than about 300 (kJ/mol)^2.[102] In this zone, the volume of N_2 adsorbed by the sample is always lower than the volume of CO_2 and decreases with increasing $(A/\beta)^2$, which is usually attributed to diffusional limitations on the N_2 adsorption

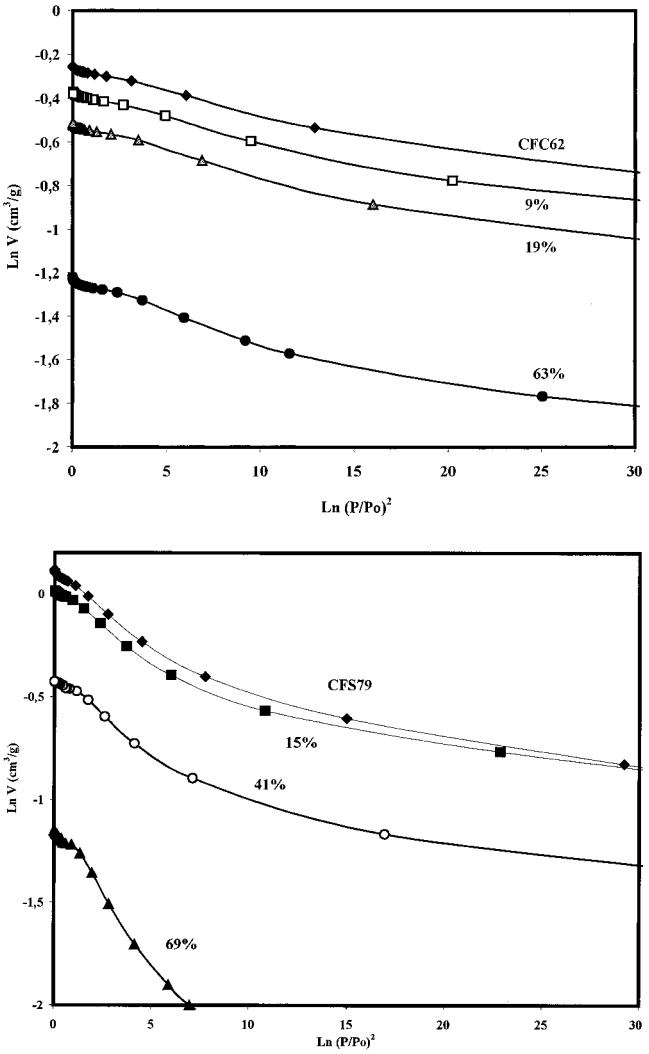

Figure 10. DR N_2 curves of ACFs at different degrees of water uptake (wt % of saturation value): sample CFC62 (a) and sample CFS79 (b).

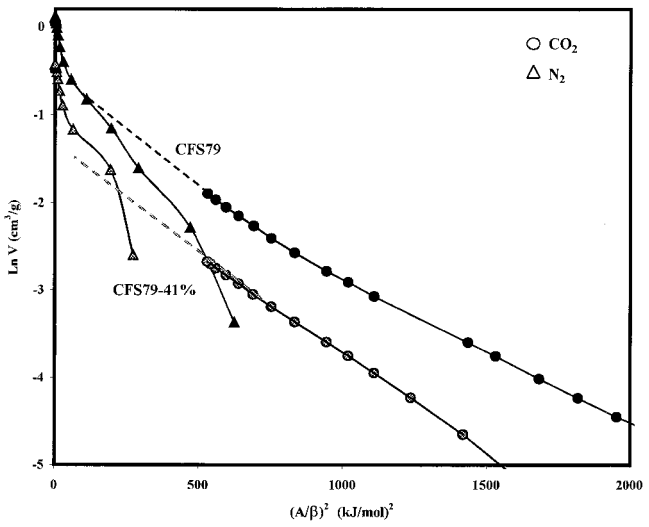

Figure 11. Characteristic curves of N_2 (77K) and CO_2 (273K) adsorption on degassed CFS79 (black) and CFS79 with water preadsorbed to 41% of the saturation value (gray).

in narrow micropores.[7] Additionally, the figure shows that the extrapolation of the CO_2 characteristic curve superimposes on the N_2 one at high relative pressures. This indicates that CO_2 adsorption reveals the narrow micropores that are included in the total micropore volume but which cannot be assessed by N_2 adsorption because of the diffusional limitations. However, there is no superposition in the curves for the 41% hydrated CFS79, and indeed, the CO_2 characteristic curve shows a significant reduction in the volumes adsorbed. This shows that water adsorbs significantly in this range of narrow microporosity, as was observed above in the analysis of the N_2 isotherms and in the calculated volumes. This result is also useful in that it supports the use of CO_2 adsorption at subatmospheric pressures and 273 K to measure the volume of narrow micropores in carbon materials.[102−104]

It is possible that this behavior could be due to the higher interaction potential existing in the narrow micropores or alternatively to a higher concentration of oxygenated surface groups associated with this microporosity. A comparison of Figures 2 and 3 shows that there is a clear relationship between the increase in the amount of oxygen groups and the increase in the supermicropore volume. This indicates that the oxygenated groups are located mainly in wide micropores, as has been observed by other researchers.[15] Therefore, water adsorption also depends strongly upon micropore potential, and these results indicate strongly that water is adsorbed in the whole of the micropore structure in a progressive way, filling the narrower micropores first.

4. Conclusions

Water adsorption in the micropore structure of ACFs is influenced by the micropore size distribution. Thus, water adsorption in carbon micropores is a physical adsorption phenomenon which, apart from the influence of the oxygen functional groups, is governed by the Lennard-Jones type of physical interaction existing between the micrographitic walls of the pores and the water molecule. This potential increases with decreasing distance between walls, as with other common adsorptives, and hence, as the pore size decreases, water adsorbs at lower relative pressures. In accordance with this process, the filling of the microporosity is progressive, the narrower micropores being filled first and water then being adsorbed in the whole range of microporosity.

This study also confirms that the water adsorbed in the micropore structure of carbon materials has a density typical of the solid-phase, i.e., around 0.92 g cm^{-3}.

Acknowledgment. J.A.-M. would like to thank The Leverhulme Trust for the award of a visiting fellowship at the University of Leeds, where part of this work was carried out. We also wish to thank project MEC-CICYT (Project-PB98-0983).

References and Notes

(1) Bansal, R. Ch.; Donnet, J.; Stoeckli, F. *Active Carbon*; Marcel Dekker: New York, 1988.

(2) Lowell, S.; Shields, J. E. *Powder, Surface Area and Porosity*, 3rd ed.; Chapman and Hall: Bristol, 1991.

(3) Jankowska, H.; Swiatkowski, A.; Choma, J. *Active Carbon*; Kemp, T. J., Ed.; Ellis Horwood: Chichester, 1991.

(4) Gregg, S. J.; Sing, S. K. W. *Adsorption, Surface Area and Porosity*, 2nd ed.; Academic Press: London, 1982.

(5) *Characterization of Porous Solids IV*; McEnaney, B., Mays, T. J., Rouquérol, J., Rodríguez-Reinoso, F., Sing, K. S. W., Unger, K. K., Eds.; Royal Society of Chemistry: London, 1997.

(6) Rouquerol, F.; Rouquerol, J.; Sing, K. *Adsorption by Powder and Porous Solids: Principles, Methodology and Applications*. Academic Press Inc: Cornwall, 1999.

(7) Rodríguez-Reinoso, F.; Linares-Solano, A. *Chemistry and Physics of Carbon;* Thrower, P., Ed.; Marcel Dekker Inc.: New York, 1988; Vol. 21, pp 2−146.

(8) Kaneko, K.; Setoyama, N.; Suzuki, T. *Characterization of Porous Solids III.*; Rouquérol, J., Rodríguez-Reinoso, F., Sing, K. S. W., Unger, K. K., Eds.; Elsevier Science Publishers B.V.: Amsterdam, 1994; p 593.

(9) Setoyama, N.; Ruike, M.; Kasu, T.; Suzuki, T.; Kaneko, K. *Langmuir* **1993**, *9*, 2612.
(10) Sosin, K. A.; Quinn, D. F. *J. Porous Mater.* **1995**, *1*, 111.
(11) Rouquerol, J. et al. *Characterization of Porous Solids III*; Rouquérol, J., Rodríguez-Reinoso, F., Sing, K. S. W., Unger, K. K., Eds.; Elsevier Science Publishers B.V.: Amsterdam, 1994; p 1.
(12) Bradley, R. H.; Rand, B. *J. Colloid Interface Sci.* **1995**, *169*, 168.
(13) Kaneko, K.; Inouke, K. *Carbon* **1986**, *8*, 772.
(14) Rodriguez-Reinoso, F.; Molina-Sabio, M.; Muñecas, M. A. *J. Phys. Chem.* **1992**, *96*, 2707.
(15) Bradley, R. H.; Rand, B. *Carbon* **1991**, *29*, 1165.
(16) Breck, D. W. *Zeolite Molecular Sieves: Structure, Chemistry, and Use*; John Wiley & Sons: New York, 1984.
(17) Barrer, R. M. *Zeolites and Clay Minerals as Sobents and Molecular Sieves*; Academic Press Inc.: London, 1978.
(18) Dubinin, M. M. *Carbon* **1980**, *18*, 355.
(19) Vartapetyan, R. Sh.; Voloshchuk, A. M. *Russ. Chem. Rev.* **1995**, *64*, 985.
(20) Dubinin, M. M.; Serpinsky, V. V. *Carbon* **1981**, *19*, 402.
(21) Dubinin, M. M.; Polyakov, N. S.; Petukhova, G. A. *Adv. Sci. Technol.* **1993**, *10*, 17.
(22) Pierce, C.; Smith, R. N. *J. Phys. Chem.* **1950**, *54*, 784.
(23) Dubinin, M. M.; Zaverina, E. D.; Serpinsky, V. V. *J. Chem. Soc.* **1955**, 1760.
(24) Dacey, J. R.; Clunie, J. C.; Thomas, D. G. *Trans. Faraday Soc.* **1958**, *54*, 250.
(25) Walker, P. L.; Janov, J. *J. Colloid Interface Sci* **1968**,*28*, 499.
(26) Barton, S. S.; Koresh, J. E. *J. Chem. Soc., Faraday Trans. 1* **1983**, *79*, 1147, 1157, 1165.
(27) Barton, S. S.; Evans, M. J. B.; Holland, J.; Koresh, J. E. *Carbon* **1984**, *22*, 265
(28) Barton , S.S.; Evans, M. J. B.; McDonald, J. A. F. *Carbon* **1991**, *29*, 1099.
(29) Evans, M. J. B. *Carbon* **1987**, *25*, 81.
(30) Evans, M. J. B.; Halliop, E.; Liang, S.; McDonald, J. A. F. *Carbon* **1998**, *36*, 1677.
(31) Morimoto, T.; Miura, K. *Langmuir* **1986**, *2*, 825.
(32) Carrott, P. J. M. *Carbon* **1991**, *29*, 507.
(33) Carrott, P. J. M.; Kenny, M. B.; Roberts, R. A.; Sing, K. S. W.; Theocharis, C. *Characterisation of Porous solids II*; Rodriguez-Reinoso, F., Rouquerol, J., Sing, K. S. W., Unger, K. K, Eds.; Elsevier: Amsterdam, 1991; p 685.
(34) Carrott, P. J. M.; Freeman, J. J. *Carbon* **1991**, *29*, 499.
(35) Carrott, P. J. M. *Carbon* **1992**, *30*, 201.
(36) Freeman, J. J.; Tomlinson, J. B.; Sing, K. S. W.; Theocharis, C. R. *Carbon* **1993**, *31*, 865.
(37) Freeman, J. J.; Tomlinson, J. B.; Sing, K. S. W.; Theocharis, C. R. *Carbon* **1995**, *33*, 795.
(38) Hall, C. R.; Holmes, R. J. *Carbon* **1992**, *30*, 173.
(39) Hall, C. R.; Holmes, R. J. *Carbon* **1993**, *31*, 881.
(40) Bradley, R. H.; Rand, B. *Carbon* **1993**, *31*, 269.
(41) Bradley, R. H. *Adv. Sci. Technol.* **1997**, *15*, 477.
(42) Salame, I. I.; Bandosz, T. *J. Colloid Interface Sci.* **1999**, *210*, 367
(43) Salame, I. I.; Bandosz, T. *Langmuir* **1999**, *15*, 587.
(44) Naono, H.; Shimoda, M.; Morita, N.; Hakuman, M.; Nakai, K.; Kondo, S. *Langmuir* **1997**, *13*, 1297.
(45) Nakai, K.; Sonoda, J.; Kondo, S.; Abe, I. *Fundamentals of Adsorption*; Suzuki, M., Ed.; Kodansha: Tokyo, 1993; p 461.
(46) Tsunoda, R. *J. Colloid Interface Sci.* **1990**, *137*, 563.
(47) Tsunoda, R.; Ozawa, T.; Ando, J. I. *J. Colloid Interface Sci.* **1998**, *205*, 265.
(48) Kaneko, K.; Kosugi, N.; Kuroda, H. *J. Chem. Soc., Faraday Trans.* **1989**, *85*, 869.
(49) Kaneko, K.; Katori, T.; Shimizu, K.; Shindo, N.; Maeda, T. *J. Chem. Soc., Faraday Trans.* **1992**, *88*, 1305.
(50) Kaneko, Y.; Ohbu, K.; Uekawa, N.; Fujie, K.; Kaneko, K. *Langmuir* **1995**, *11*, 708.
(51) Youssef, A. M.; El-Khouly, A. A.; Ahmed, A. I.; El-Shafey, E. I. *Adv. Sci. Technol.* **1995**, *12*, 211.
(52) Turov, V. V.; Leboda, R. *Adv. Sci. Technol.* **1998**, *16*, 837.
(53) Foley, N. J.; Thomas, K. M.; Forshaw, P. L.; Stanton, D.; Norman, P. R. *Langmuir* **1997**, *13*, 2083.
(54) Lee, W. H.; Reucroft, P. J. *Carbon* **1999**, *37*, 7.
(55) Stoeckli, F.; Kraehenbuehl, K.; Morel, D. *Carbon* **1983**, *21*, 589.
(56) Carrasco-Marín, F.; Mueden, A.; Centeno, T. A.; Stoeckli, F.; Moreno-Castilla, C. *J. Chem. Soc., Faraday Trans.* **1997**, *93*, 2211.
(57) Wintgens, D.; Lavanchy, A.; Stoceckli, F. *Adv. Sci. Technol.* **1999**, *17*, 761.
(58) Stoeckli, F.; Lavanchy, A. *Carbon* **2000**, *38*, 475.
(59) López-Ramón, M. V.; Stoeckli, F.; Moreno-Castilla, C.; Carrasco-Marín, F. *Carbon* **2000**, *38*, 825.
(60) Antochenko, V. Y.; Davidov, A. S.; Ilyin, V. V. *Physics of Water*; Naukova Dumka: Kiev, 1991.
(61) Segarra, E. I.; Glandt, E. D. *Chem. Eng. Sci.* **1994**, *49*, 2953.
(62) Ulberg, D. E.; Gubbins, K. E. *Mol. Phys.* **1995**, *84*, 1139.
(63) Maddox, M.; Ulberg, D. E.; Gubbins, K. E. *Fluid Phase Equilibria* **1995**, *104*, 145.
(64) Talu, O.; Meunier, F. *AIChE J.* **1996**, *42*, 809.
(65) Aksenenko, E. V.; Tarasevich, Y. I. *Adv. Sci. Technol.* **1996**, *14*, 383.
(66) Tarasevich, Y. I.; Zhukova, A. I.; Aksenenko, E. V.; Bondarenko, S. V. *Adv. Sci. Technol.* **1997**, *15*, 497.
(67) Müller. E. A.; Rull, L. F.; Vega, L. F.; Gubbins, K. E. *J. Phys. Chem.* **1996**, *100*, 1189.
(68) Müller, E. A.; Gubbins, K. E. *Carbon* **1998**, *36*, 1433.
(69) McCallum, C. L.; Bandosz, T. J.; McGrother, S. C.; Müller, E. A.; Gubbins, K. E. *Langmuir* **1999**, *15*, 533.
(70) Do, D. D.; Do, H. D. *Carbon* **2000**, *38*, 767.
(71) Kaneko, K. *Carbon* **2000**, *38*, 387.
(72) Iiyama, T.; Nishikawa, K.; Otowa, T.; Suzuki, T.; Kaneko, K. *J. Phys. Chem.* **1995**, *99*, 10075.
(73) Iiyama, T.; Nishikawa, K.; Suzuki, T.; Kaneko, K. *Chem. Phys. Lett.* **1997**, *274*, 152.
(74) Iiyama, T.; Nishikawa, K.; Otowa, T.; Suzuki, T.; Kaneko, K. *Characterisation of porous solids IV*; McEnaney, B., May, T. J., Rouquerol, J., Rodriguez-Reinoso, F., Sing, K. S. W., Unger, K. K. K., Eds.; Royal Society of Chemistry: London, 1998; p 41.
(75) Iiyama, T.; Ruike, M.; Suzuki, T.; Kaneko, K. *Characterisation of porous solids V*; Unger, K. K. K., Kreysa, G., Baselt, J. P., Eds.; Elsevier Science: Amsterdam, 2000; p 355.
(76) Dubinin, M. M.; Raduskevich, L. V. *Proc. Acad. Sci. SSSR* **1947**, *55*, 331.
(77) Sing, K. S. W.; Everett, D. H.; Haul, R. A. W.; Moscou, L.; Pierotti, R. A.; Rouquerol, J.; Siemieniewska, T. *Pure Appl. Chem.* **1985**, *57*, 603.
(78) Alcañiz-Monge, J.; Cazorla-Amorós, D.; Linares-Solano, A.; Yoshida, S.; Oya, A. *Carbon* **1994**, *32*, 1277.
(79) Alcañiz-Monge, J.; Cazorla-Amorós, D.; Linares-Solano, A. *Carbon* **1997**, *35*, 1665.
(80) Román-Martínez, M. C.; Cazorla-Amorós, D.; Linares-Solano, A.; Salinas-Martínez de Lecea, C. *Carbon* **1993**, *31*, 895.
(81) Bohem, H. P.; Voll, M. *Carbon* **1970**, *8*, 227.
(82) Raymundo-Piñero, E.; Cazorla-Amorós, D.; Salinas-Martínez de Lecea, C.; Linares-Solano, A. *Carbon* **2000**, *38*, 383.
(83) Young, D. H.; Crowell, A. O. *Physical Adsorption of Gases*; Butterworth: London, 1962.
(84) Balbuena, P. B.; Gubbins, K. E. *Langmuir* **1993**, *9*, 1801.
(85) Stoeckli, F.; Jakubov, T.; Lavanchy. A. *J. Chem. Soc., Faraday Trans.* **1994**, *90*, 783.
(86) Kenny, M. B.; Roberts, R. A.; Sing, K. S. W. *Extended Abstracts of Carbone '90*; Grenie, Y., Ed.; Grupe Francais D'Etude des Carbones: Paris, 1990; p 10.
(87) Sing, K. S. W. *Characterization of Powder Surfaces*; Parfitt, G. D., Sing, K. S. W., Eds.; Academic Press: London, 1975.
(88) Kiselev, A. V.; Yashin, Y. I. *Gas-Adsorption Chromatography*; Plenum Press: New York, 1969.
(89) Curthoys, G.; Davydov, V. Y.; Kiselev, A. V.; Kiselev, S. A.; Kuznetsov, B. V. *J. Colloid Interface Sci.* **1974**, *48*, 58.
(90) Hassan, N. M.; Ghosh, T. K.; Hines, A. L.; Loyalka, S. K. *Carbon* **1991**, *29*, 681.
(91) Barton, S. S.; Koresh, J. E. *Carbon* **1984**, *22*, 481.
(92) Inspektor, A.; Koresh, J. E.; Barton, S. S.; Evans, M. J. B. *Carbon* **1986**, *24*, 325.
(93) Stoeckli, F.; Huguenin, D. J. *Chem. Soc., Faraday Trans.* **1992**, *88*, 737.
(94) Suzuki, M.; Doi, H. *Carbon* **1982**, *20*, 441.
(95) O'Koye, I. P.; Benham, M.; Thomas, K. M. *Langmuir* **1997**, *13*, 4054.
(96) Verma, S. K.; Walker, P. L. *Carbon* **1990**, *28*, 175.
(97) Hennig, G. R. *J. Chem. Phys.* **1961**, *58*, 12.
(98) Bellissent-funel, M. C.; Sridi-Dorbez, R.; Bosio, L. *J. Chem. Phys.* **1996**, *104*, 10023.
(99) Kaneko, K.; Hanzawa, Y.; Liyama, T.; Kanda, T.; Suzuki, T. *Adsorption* **1999**, *5*, 7.
(100) Watanabe, A.; Liyama, T.; Kaneko, K. *Int. Symp. Carbon*; Carbon Society Japan: Tokyo, 1998; p 624.
(101) Kaneko, K.; Miyawaki, J.; Watanabe, A.; Suzuki, T. *Fundamentals of Adsorption*; Mneunier, F., Ed.; Elsevier: Amsterdam, 1998; p 51.
(102) Cazorla-Amorós, D.; Alcañiz-Monge, J.; Linares-Solano, A. *Langmuir* **1996**, *12*, 2820.
(103) Cazorla-Amorós, D.; Alcañiz-Monge, J.; de la Casa-Lillo, M. A.; Linares-Solano, A. *Langmuir* **1998**, *14*, 4589.
(104) Linares-Solano, A.; Salinas-Martínez de Lecea, C.; Alcañiz-Monge, J.; Cazorla-Amorós, D. *Tanso* **1998**, *185*, 316.